Organic Electronics 13 (2012) 833–839

Contents lists available at SciVerse ScienceDirect

Organic Electronics

journal homepage: www.elsevier.com/locate/orgel

Enhanced efficiency of organic light emitting devices (OLEDs) by control of laser imaging condition

Sang Hee Cho [a], Seung Mook Lee [b], Min Chul Suh [a,*]

[a] Department of Information Display, Kyung Hee University, Dongdaemoon-Gu, Seoul 130-701, Republic of Korea
[b] Samsung Mobile Display Co., Ltd., San #24 Nongseo-Dong, Giheung-Gu, Yongin-City, Gyeonggi-Do 446-711, Republic of Korea

ARTICLE INFO

Article history:
Received 21 November 2011
Received in revised form 19 January 2012
Accepted 22 January 2012
Available online 8 February 2012

Keywords:
Laser Induced Thermal Imaging (LITI)
Deterioration
Interface
Dwell time control

ABSTRACT

Laser Induced Thermal Imaging (LITI) is a laser addressed thermal patterning technology with unique advantages such as excellent uniformity of transfer film thickness, capability of multilayer stack transfer, high resolution and scalability to large-size mother glass. However, the deterioration of the device performance during imaging process has been an obstacle to use it as a commercial technology. To investigate a possibility of thermal deformation of organic materials as a transfer layer and a receptor layer during imaging process, we executed a preliminary annealing test by using standard green devices at various temperatures. By comparison of these results with those obtained from LITI devices, we found that the main reason of device deterioration could be originated from the mobility change of the organic layers. Hence, we developed the dwell time control technology to suppress the thermal impact during LITI process and we finally obtained current efficiency which is quite equivalent to that obtained from the standard evaporation devices.

1. Introduction

An increasing interest in organic light-emitting devices (OLEDs) has led to a very large research effort towards the development of new materials [1–3] and/or device architectures [4–9] to improve the device performances such as brightness, efficiency, lifetime, etc. One of the major limitations to the realization of a patterned full color OLEDs is the lack of a simple, low-cost method for patterning thin organic molecular layers. The use of conventional photolithography is difficult to apply to the fabrication of full color OLEDs because many organic thin films are susceptible to damage during exposure to wet etchant, developer, stripper, etc. Thus, several alternative patterning methods have been demonstrated: the use of excimer laser ablation [10–12], ink-jet printing [13–15], and micro-patterning by cold welding [16,17]. A more recent and viable method for patterning full color OLEDs may be a Laser-Induced Thermal Imaging (LITI) process [18–20]. However, organic materials as donor and/or receptor layers can be deformed because it is the process which basically utilizes the thermal energy for patterning. Hence the heat transfer from the thermally expanded area may cause a change of physical property of organic material which results in a poor reproducibility as well as serious deterioration of device performance [21] as shown in Fig. 1. Associated with this problem, synthesis of new materials for hole transport layer (HTL) and emitting layer (EML) with high thermal stability has become very important because the EML and optical path layer could normally be transferred simultaneously after multi-stacked deposition on the donor film as reported by Chin [19]. However, it normally takes too long time to obtain totally new material sets because there is no guideline of synthetic parameters of the materials for LITI process [e.g. glass transition temperature (T_g), molecular weight (M_w), surface energy, etc.]. Thus, a more convenient approach to suppress the thermal deformation by control of the process parameters is necessary. In this study, we present about the phenomenon of thermal deformation of the materials and a facile methodology to reduce it during laser transfer process.

* Corresponding author. Tel.: +82 2 961 0694; fax: +82 2 968 6924.
E-mail address: mcsuh@khu.ac.kr (M.C. Suh).

1566-1199/$ - see front matter © 2012 Elsevier B.V. All rights reserved.
doi:10.1016/j.orgel.2012.01.023

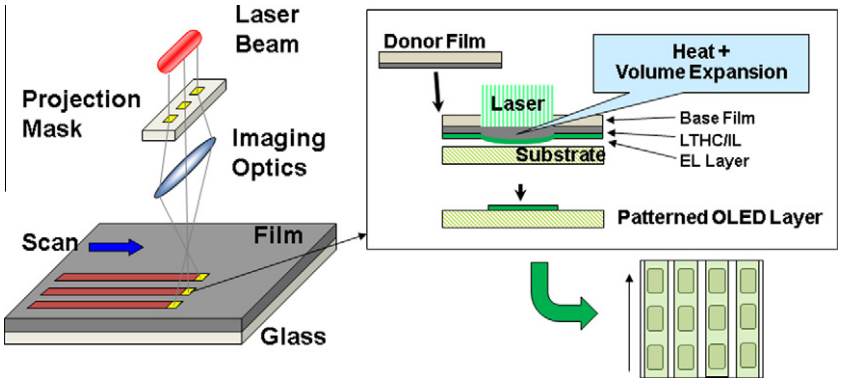

Fig. 1. Schematic diagram of laser imaging experimental setup.

2. Experimental

Materials: A commercially available material called IDE406 (HTM) as a hole injection layer or hole transport layer (manufactured by Idemitsu Kosan), 1,4,5,8,9,11-hexaazatriphenylene-hexacarbonitrile (HAT-CN) as a π-electron acceptor (manufactured by LG Chem.), 9,10-di(2-naphtyl) anthracene (ADN) based materials as a fluorescent green host (GGH01, manufactured by Gracel) and green dopant (GGD01, manufactured by Gracel) for an emitting layer, LGC 201 as an electron transport layer (manufactured by LG Chem.), lithium quinolate (LiQ) as a π-electron donor and/or electron injection layer were purchased used without purification.

Device fabrication: To fabricate OLED devices, clean glass substrates precoated with indium tin oxide (ITO)/silver (Ag)/ITO layers were used to investigate top emission properties. Line patterns of anode materials were formed on glass by photolithography process. The ITO glasses were cleaned by sonification in an isopropyl alcohol and acetone, rinsed in deionized water, and finally irradiated in a UV-ozone chamber. All organic materials were deposited by the vacuum evaporation technique under a pressure of $\sim 1 \times 10^{-7}$ Torr. The deposition rate of organic layers was about 1 Å/s. For LITI devices, HIL and HTL were deposited on a glass substrate with reflective anode. Then, HTL and EML was successively deposited on a poly(ethyleneterephthalate) (PET) donor film with a light to heat conversion layer (LTHC) and interlayer (IL) at a thickness of ~80 nm thin film. After lamination of donor film with transfer layers, the laser imaging was conducted by using laser beam (wavelength of laser beam: 1064 nm) generated by Nd:YAG laser. After formation of patterned HTL/EML, LGC201 was deposited on the substrate with HIL/HTL//patterned HTL/EML// as an ETL [where, the double slash ("//") indicates the interface between the organic layer formed by evaporation process and by LITI process]. Then, LiQ and Mg/Ag were deposited in another vacuum deposition system without breaking vacuum. Deposition rates of LiQ and Mg/Ag were 0.5 and 0.1 Å/s, respectively. As a result, we could obtain the top-emitting microcavity OLED structure as follows: [ITO/Ag/ITO/HTM:HAT-CN (142 nm, 3%)//HTM (30 nm)/GGH01:GGD01 (3%, 40 nm)//LGC201:LiQ (37 nm, 50%)/LiQ (1.5 nm)/Mg:Ag (14 nm, 10%)] (Fig. 2).

Measurements: The current density–voltage (*J*–*V*) and luminance–voltage (*L*–*V*) data of OLEDs were measured by Keithley SMU 238 and Minolta CS-100A, respectively. The OLED area was 4 mm^2 for all the samples studied in this work. Electroluminescence (EL) spectra and CIE coordinate were obtained using a Photoresearch PR-650 spectroradiometer.

3. Results and discussion

3.1. Laser patterning process

In principle, the LITI process utilizes a donor film, a highly accurate laser exposure system, and a substrate. The donor film consists of a transparent base film with a few coating layers as shown in Figs. 1 and 2. The base film is typically a polyester film such as a PET film. The layer adjacent to the base film is a LTHC layer which converts the laser energy to heat. The LTHC layer comprises a material which absorbs the wavelength of irradiation and converts the portion of an incident radiation into sufficient heat to enable the thermal transfer of the materials from the donor (film) to the receptor (substrate). Typically, LTHC layers are absorptive in the infrared region of the electromagnetic spectrum.

It is generally desirable for the radiation absorber to be highly absorptive of the imaging radiation, enabling an optical density at the wavelength of the imaging radiation (1064 nm for this study) in the range of 1.0–2.0 using a minimum amount of radiation absorber to be used. Dyes absorbing in the IR region of the spectrum and pigment materials such as carbon black and graphite can be used as LTHC layers. From this technology, we could typically transfer a 50–135 nm thick HTL/EML layers. Very interestingly, the transfer layer can be comprised by multiple layers (e.g. HTL + EML) because LITI process is basically bulk transfer, not sublimation transfer method such as Radiation Induced Sublimation Transfer (RIST) or Laser Induced Patternwise Sublimation (LIPS) [22,23]. However, the donor film is necessary to be put in close contact with a substrate by a vacuum suction tool and exposed with the laser system. As shown in Fig. 1, the laser irradiation apparatus normally includes a laser generator, a patterned mask, and a projection lens. The laser generator is constituted by

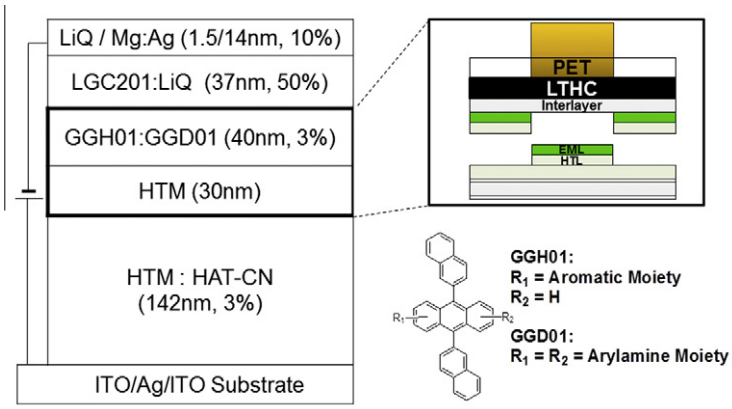

Fig. 2. The structures of fabricated OLEDs (the green top-emitting fluorescent OLED for LITI experiments). (For interpretation of the references to colour in this figure legend, the reader is referred to the web version of this article.)

continuous wave (CW) Nd:YAG laser, which irradiates a laser beam on a predetermined region of the donor substrate, and performs scanning in an arrow direction. In this case, the laser beam irradiated from the laser generator passes through the open-transparent area of patterned mask and the transmitted laser beam is focused by the projection lens and then irradiated on the donor substrate. The laser beam could be additionally shielded for the region where the patterning is not necessary by additional shadow masking on top of receptor substrate. The vacuum chuck for the substrate was attached to one dimensional translation stage such that it could be scanned in the plane of the donor/receptor surface, allowing laser exposure over the entire surface. When the LTHC is exposed by laser from the back-side of donor film, the exposed area is heated very rapidly (up to $\sim 7 \times 10^7$ °C/s) to cause an abrupt volume expansion in between transfer layer and base film which is the driving force of thermal transfer process. From this reason, the temperatures of interface between PET and LTHC layer reaches up to 100–200 °C, albeit for very short time-periods in the μs to ms range [24]. Meanwhile, Gong et al. asserted that the molecular aggregation of the dopant molecules in host molecular system at higher temperatures might be one of the important causes of OLED decay, which may result in an ineffective host–guest energy transfer [25]. Hence, the suppression of an excessive temperature rise during this process may be very important to obtain the good performance of OLED devices although the temperature elevation to a certain degree is inevitable to realize a laser transfer.

3.2. Simulated thermal annealing test of transfer layer

To investigate a change of physical properties of transfer layer, we performed a simulated annealing experiment for the materials which is transferred during process. The structure of the hole only devices (HOD) we fabricated are as follows:

HOD 1: ITO/MoO_3 (1 nm)/HTM (100 nm)/MoO_3 (10 nm)/Al (100 nm).
HOD 2: ITO/MoO_3 (1 nm)/GGH01 (100 nm)/MoO_3 (10 nm)/Al (100 nm).
HOD 3: ITO/MoO_3 (1 nm)/GGD01 (100 nm)/MoO_3 (10 nm)/Al (100 nm).

We investigated the *J–V* curves of a device prepared without any annealing and the devices fabricated after thermal annealing processes at the temperature range of 100–175 °C (in the glove box; O_2 and H_2O contents < 10 ppm; for 30 min). From this experiment, we could not obtain any evidence associated with a thermal deformation of HTM (HOD 1) as shown in Fig. 3(a). In other words, all the *J–V* curves collected from the HOD 1 fabricated by a simulated annealing test were very similar and almost over-laid in the error range. In contrast, there was a very reliable tendency upon thermal annealing processes of GGH01 and GGD01 molecules. In most cases, the current density was gradually increased by 1–1.5 order of magnitude upon thermal annealing from 100 to 150 °C for HOD 2 and 3 as shown in Fig. 3(b) and (c). However, the current density was somewhat decreased after annealing at 175 °C in case of HOD 2 presumably due to a beginning of a certain phase change, while HOD 3 showed increased current density behavior even at this condition.

Hence we could conclude that the recombination zone inside EML may be shifted toward cathode side which causes an exciton quenching or many other non-radiative processes upon thermal annealing process at the temperature range of 100–150 °C (Fig. 4). Therefore, the process to pattern an EML should be performed at low temperature to obtain high efficiency. Consequently, we have to find an appropriate method to suppress the temperature increase during laser imaging process.

3.3. Control of the laser intensity

In general, the laser intensity could be controlled by varying two parameters as follows: (i) laser scan speed, and (ii) laser power, in accordance with an Eq. (1). The most difficult thing is the fact that the pattern quality and device performance are normally in the relationship

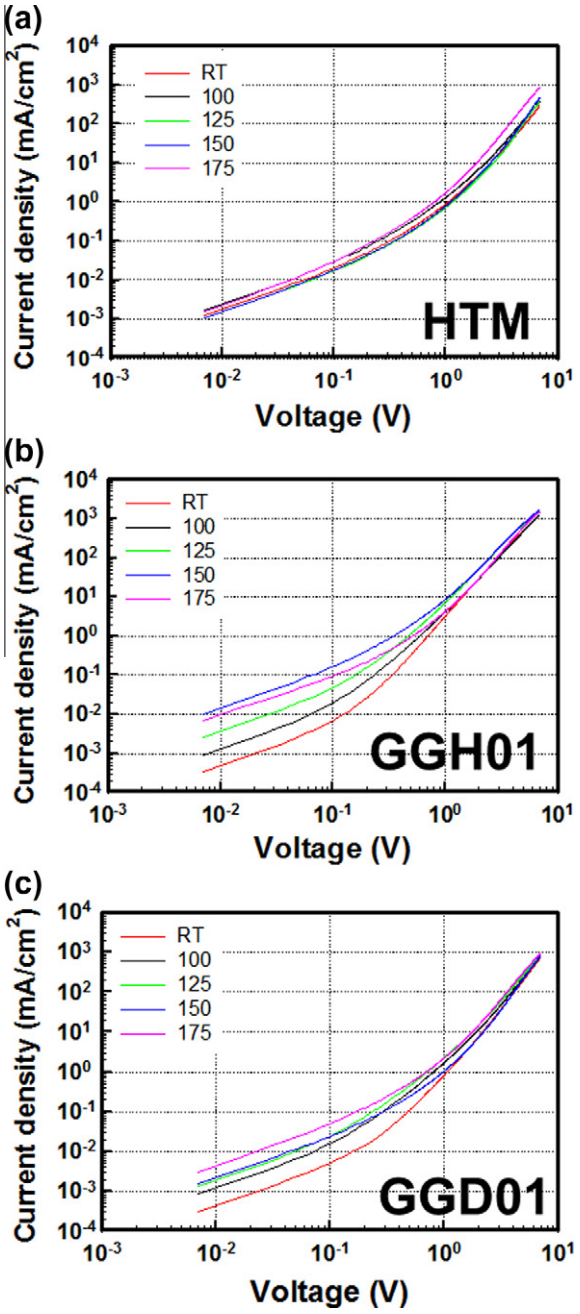

Fig. 3. The structures of the hole only devices (HOD) for HTM, GGH01 and GGD01 materials for the thermal annealing experiment.

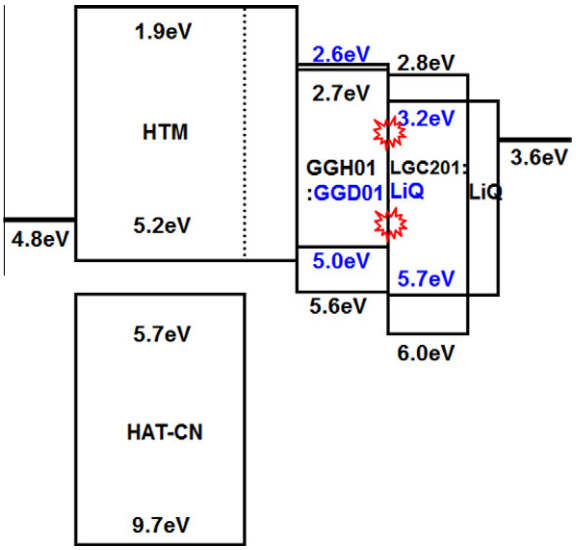

Fig. 4. Energy diagram of fabricated devices.

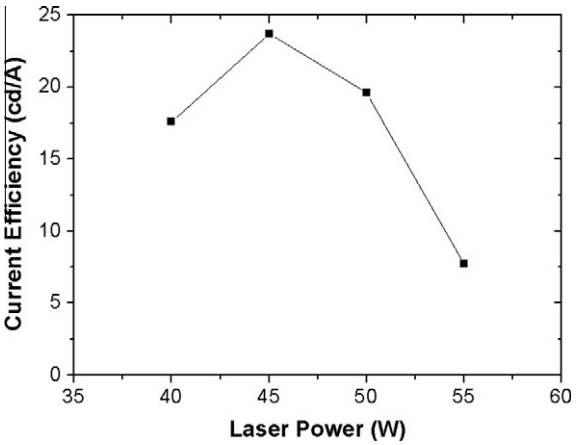

Fig. 5. The relationship of current efficiency vs. laser power for fabrication of devices by LITI process.

of inverse proportion. For example, we can obtain very nice pattern quality with poor device performances if we prepare the LITI device at relatively slow scan speed. However, if the scan speed is too slow, the current efficiency cannot be reached up to similar level of that obtained from evaporation reference. Hence we normally control the scan speed with varying the laser power simultaneously. Nevertheless, the process window in accordance with a laser power at a certain scan speed is rather narrow as shown in Fig. 5. For example, the maximum current efficiency of 23.7 cd/A was obtained when the scan speed and laser power were 0.3 m/s and 45 W by using laser beam size of $200 \times 125\ \mu m^2$ (cf. evaporation reference: 49.2 cd/A). Thus, we need to control the laser intensity much more minutely for suppression of deterioration of device performance. Thus, we investigated the possible parameters which may affect the device performance as follows: first, we took into account of two main parameters which can typically be correlated to an energy density (or dosage) of laser beam as shown in Eq. (1):

$$\text{Energy density(Dosage)} = [P/(a \times b)] \times (a/v)\ [\text{J/cm}^2] \quad (1)$$

where the P is a laser power, the a and b is the length and width of laser beam after transit through the open area of projection mask, respectively. The v is a laser scan speed.

Energy density can also be divided into two parts as follows:

The first part in Eq. (1) is a "power density" of laser source, which is estimated from the laser power per unit area as shown in Eq. (2). Here, "*b*" is a constant because it is normally fixed when the display format is determined as a "sub-pixel pitch":

$$\text{Power density} = P/(a \times b)\ [\text{Watt(or J/s)/cm}^2] \quad (2)$$

And, the second part in Eq. (1) is related to a "dwell time" of a focused laser beam at the certain position during laser scanning, which is very important factor to improve device performance as well as pattern quality. This is very interesting factor because "*a*" could be ostensibly eliminated from the Eq. (1):

$$\text{Dwell time} = a/v\ [\text{cm}/(\text{cm/s})] \quad (3)$$

In some aspect, a spot size (or unit area) of laser beam may be very important for a LITI process because it may be associated with a unit or initial volume which might be very hot initially and may be propagated along a scan direction (Fig. 6). Hence this unit area is kinetically very important because the latent heat in this area will affect the thermal deformation of EML and/or HTL during LITI process.

To evaluate an importance of this parameters, we prepared three different types of projection masks to irradiate laser beam with different spot size on the donor film [laser beam size: length (*a*): 50, 100 and 200 μm; width (*b*): 125 μm] as shown in Fig. 6. The Devices A, B, and C with structures of ITO/Ag/ITO/HTM:HAT-CN (142 nm, 3%)// HTM (30 nm)/GGH01:GGD01 (3%, 40 nm)//LGC201:LiQ (37 nm, 50%)/LiQ (1.5 nm)/Mg:Ag (14 nm, 10%) were employed for this evaluation (Fig. 4). As following Table 1, Device A was prepared at scan speed of 0.7 m/s with dwell time of 286 μs (laser beam size: 200 × 125 μm^2); Device B was prepared at scan speed of 0.7 m/s with dwell time of 143 μs (laser beam size: 100 × 125 μm^2); Device C was prepared at scan speed of 0.5 m/s with dwell time of 100 μs (laser beam size: 50 × 125 μm^2).

Fig. 7(a) shows the *J*–*V* and *L*–*V* characteristics of fabricated green OLEDs. At a given constant voltage of 5.0 V, current density values of 13.08, 0.61, 45.76, and 13.83 mA/cm^2 were observed in the fabricated devices (Reference, A, B, and C). The driving voltage to reach 1000 cd/m^2 was 4.04 V for the Reference, 3.78 V for Device A, 3.82 V for the Device B, and 4.16 V for the Device C, respectively (Table 1). Interestingly, the Device A prepared at a scan speed of 0.7 m/s with a longer dwell time (286 μs) showed relatively lower current density throughout the whole scan range (−2 to 7 V) maybe due to a molecular disordering of the organic layers which may cause a mobility drop. In other words, there could be a molecular reorientation during laser imaging process if the dwell time is too long (~286 μs) and the resultant molecular disordering could reduce a bulk mobility of a certain layer. This might be very similar phenomenon to that caused from the excessive thermal annealing experiment of GGH01 over

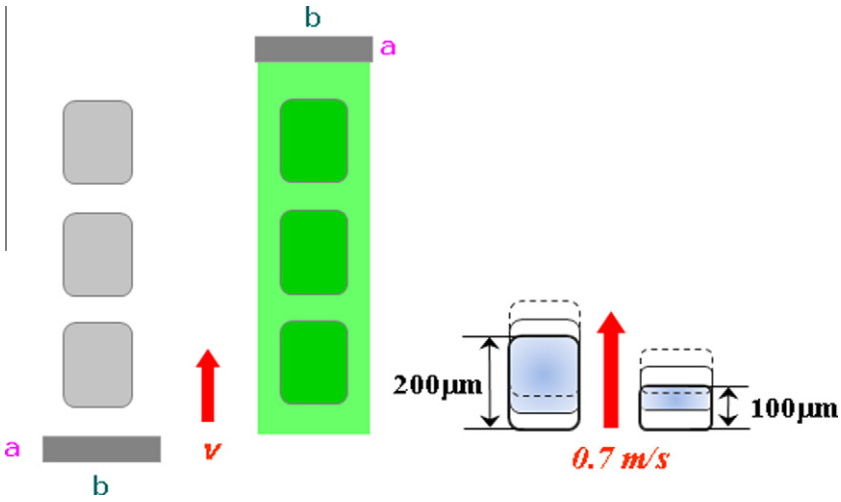

Fig. 6. The three different dwell time conditions were tried by changing the length of the laser beam ("a"); the width of laser beam ("b") was fixed to 125 μm because it is related to a sub-pixel pitch of the devices. The laser scan speed ("v") was varied from 0.5 m/s to 0.7 m/s (see also Table 1).

Table 1
Performances of the green OLED Devices fabricated by LITI Process.

Device	Scan speed (m/s)	Length of laser beam (μm)	Dwell time (μs)	Current efficiency (Cd/A)	Operating voltage (V) @1000 nits	Operating voltage (V) @8000 nits
Ref.	–	–	–	48.0 (49.2)[a]	4.04	5.00
A	0.7	200	286	12.8 (12.9)[a]	3.78	5.40
B	0.7	100	143	17.2 (17.5)[a]	3.82	5.00
C	0.5	50	100	38.6 (43.9)[a]	4.16	5.10

[a] The current efficiency in the parenthesis is the maximum current efficiency.

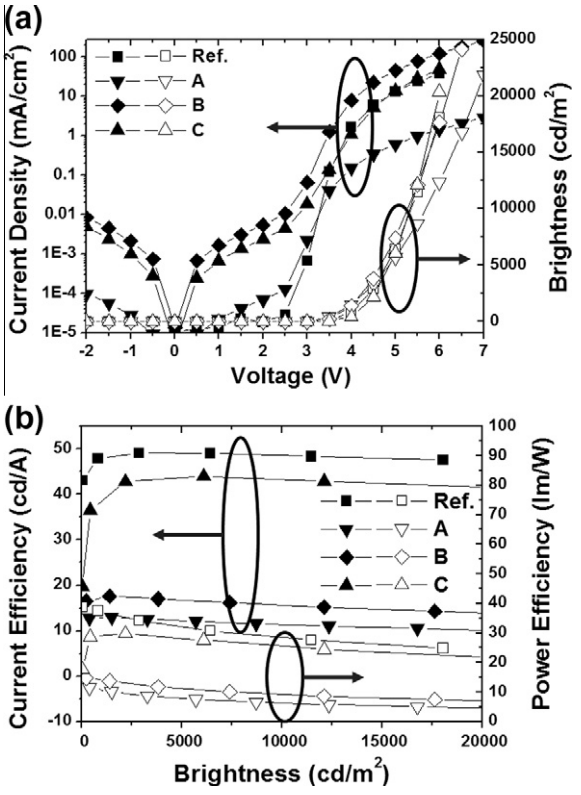

Fig. 7. (a) *J–V–L*, (b) current and power efficiency characteristics of the fabricated fluorescent green OLEDs.

than 175 °C as shown in Fig. 3(b) [26,27]. Because of this reason, we could observe the serious current density lowering in the Device A. Conversely, the Device B prepared at a same scan speed (0.7 m/s) with a shorter dwell time (143 μs) showed greater current density plausibly due to a mobility enhancement originated by a partial molecular ordering or aggregation as a moderate thermal annealing effect during laser imaging process. In other words, we could presume that the temperature may be raised over than 175 °C for Device A and less than 150 °C for Device B although we cannot expect an exact temperature in this process because the dwell time is too short to be correlated. However, the devices obtained by laser imaging process in these conditions showed different tendency of operating voltage at 1000 cd/m^2 (operating voltage: Device C > Device B > Device A). But, the operating voltage at relatively higher brightness region (~8000 cd/m^2) showed same tendency (operating voltage: Device A > Device C > Device B). In other words, the operating voltage may be increased if the mobility drops seriously, plausibly due to a molecular disordering aforementioned. As a result, the operating voltage to reach 8000 cd/m^2 was 5.0 V for Reference, 5.4 for Device A, 5.0 for Device B, 5.1 V for Device C, respectively. Besides, the other problem of such devices obtained by LITI process might be their high leakage current level. In other words, they normally show higher leakage current level than that of reference device maybe due to a thinning in places of EML layer originated from melt-and-stick type scan propagation process. Therefore, an EL images of Device A and B were not that uniform due to this thermal effect during laser imaging process (Fig. 8). Unfortunately, the pixel brightness non-uniformity originated from this reason cannot be perfectly removed only by control of dwell time. This issue could be solved by the development of EML with high thermal stability and/or with totally disordered amorphous structure. Anyhow, the slower laser scan speed of 0.5 m/s gave much better pattern quality although the potential of temperature rise is much higher. Instead, we applied very short dwell time condition of about 100 μs with this slower laser scan speed (0.5 m/s) (Device C) and we finally obtained very similar current density value of ~13.83 mA/cm^2 compared to ~13.08 mA/cm^2 of reference device although the leakage current level of Device C was still very higher.

The current and power efficiency characteristics of fabricated OLEDs are shown in Fig. 7(b). At a given constant luminance of 1000 cd/m^2, the current and power efficiencies were 48.0 cd/A and 37.3 lm/W for the Reference Device, 12.8 cd/A and 10.6 lm/W for the Device A, 17.2 cd/A and 14.1 lm/W for the Device B, and 38.6 cd/A and 29.1 lm/W for the Device C, respectively. The maximum current and power efficiencies were 49.2 cd/A and 38.7

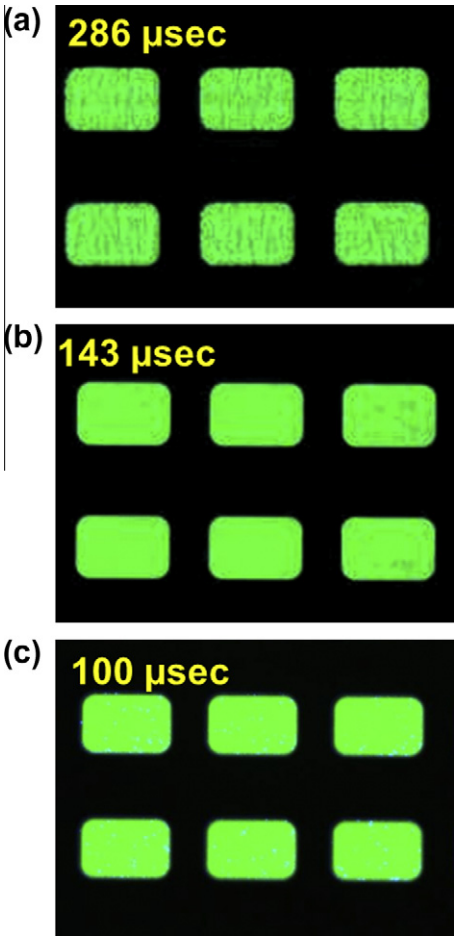

Fig. 8. EL microscopic images of OLED devices prepared by different dwell time conditions: (a) 286 μs, (b) 143 μs, and (c) 100 μs, respectively.

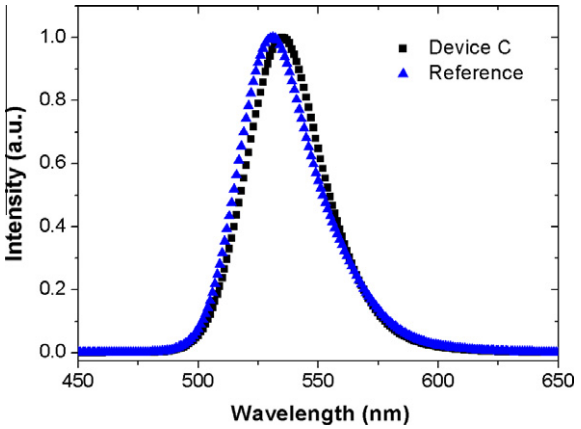

Fig. 9. The electroluminescent spectra of Reference and Device C.

lm/W for the Reference device, 12.9 cd/A and 11.5 lm/W for the Device A, 17.5 cd/A and 14.8 lm/W for the Device B, and 43.9 cd/A and 29.9 lm/W for the Device C, respectively. The best efficiency was obtained from the Device C among the devices fabricated by LITI process (at 1000 cd/m^2). But, Device C showed rather higher operating voltage behavior although it gave very good current efficiency as well as power efficiency. These data were also summarized in Table 1. In addition, we showed EL microscopic images of those OLED devices prepared by different dwell time conditions in Fig. 8.

Fig. 9 shows the electroluminescent spectra of resultant green OLED (Device C) and evaporation reference. Both devices showed very narrow green emission at ~532–535 nm due to a strong microcavity effect. The color coordinates (CIE 1931) were obtained as (0.25, 0.71) for the Device C while the evaporation reference showed (0.22, 0.74) which means that the total thickness was different for each device. However, there were no side peaks or shoulder which means that the perfect energy transfer was realized from this device architecture and processes.

4. Conclusions

We found that the dwell time control is very important to improve a device efficiency of laser patterned devices (by LITI process). The appropriate selection of unit scan length of laser beam is known to be very important parameter to suppress the thermal damage during laser transfer process along with a scan speed. From this methodology, we obtained decently high current efficiency up to 43.9 cd/A compared to that of evaporation reference device (49.2 cd/A).

Acknowledgments

This work was supported by the Basic Science Research Program through the National Research Foundation of Korea (NRF) funded by the Ministry of Education, Science and Technology (Grant No. NRF-2011-0006847). This research was also supported by Samsung Mobile Display – KHU OLED Research Center (Grant No. 20111029).

References

[1] M.A. Baldo, D.F. O'Brien, Y. You, A. Shoustikov, S. Sibley, M.E. Thompson, S.R. Forrest, Nature 395 (1998) 151.
[2] S. Lamansky, P. Djurovich, D. Murphy, F. Abdel-Razzaq, H.-E. Lee, C. Adachi, P.E. Burrows, S.R. Forrest, J. Am. Chem. Soc. 123 (2001) 4304.
[3] K. Walzer, B. Maennig, M. Pfeiffer, K. Leo, Chem. Rev. 107 (2007) 1233.
[4] C. Adachi, M.E. Thompson, S.R. Forrest, IEEE J. Sel. Top. Quantum Electron 8 (2002) 372.
[5] S. Tokito, T. Iijima, Y. Suzuri, H. Kita, T. Tsuzuki, F. Sato, Appl. Phys. Lett. 83 (2003) 569.
[6] W.S. Jeon, T.J. Park, S.Y. Kim, R. Pode, J. Jang, J.H. Kwon, Appl. Phys. Lett. 93 (2008) 063303.
[7] S.H. Kim, J. Jang, J.Y. Lee, Appl. Phys. Lett. 91 (2007) 083511.
[8] M. Ikai, S. Tokito, Y. Sakamoto, T. Suzuki, Y. Taga, Appl. Phys. Lett. 79 (2001) 156.
[9] S. Watanabe, N. Ide, J. Kido, Jpn. J. Appl. Phys. 46 (2007) 1186.
[10] S. Noach, E.Z. Faraggi, G. Cohen, Y. Avny, R. Neumann, D. Davidov, A. Lewis, Appl. Phys. Lett. 69 (1996) 3650.
[11] E.W. Ellis, D.M. Foley, D.R. Arnold, U.S. Patent 5 (171) (1992) 650.
[12] M. Boroson, L. Tutt, K. Nguyen, D. Preuss, M. Culver, G. Phelan, SID Int. Symp. Dig. Tech. Papers 16 (2005) 972.
[13] T.R. Hebner, C.C. Wu, D. Marcy, M.H. Lu, J.C. Sturm, Appl. Phys. Lett. 72 (1998) 519.
[14] J. Bharathan, Y. Yang, Appl. Phys. Lett. 72 (1998) 2660.
[15] S.-C. Chang, J. Liu, J. Bharathan, Y. Yang, J. Onohara, J. Kido, Adv. Mater. 11 (1999) 734.
[16] C. Kim, P.E. Burrows, S.R. Forrest, Science 288 (2000) 381.
[17] S.R. Forrest, Nature 428 (2004) 911.
[18] M.C. Suh, B.D. Chin, M.-H. Kim, T.M. Kang, S.T. Lee, Adv. Mater. 15 (2003) 1254.
[19] B.D. Chin, J. Phys. D: Appl. Phys. 40 (2007) 5541.
[20] M.B. Wolk, S. Lamansky, W.A. Tolbert, SID Int. Symp. Dig. Tech. Papers. 39 (2008) 511.
[21] M.C. Suh, T.M. Kang, S.W. Cho, Y.G. Kwon, H.D. Kim, H.K. Chung, SID Int. Symp. Dig. Tech. Papers. 40 (2009) 794.
[22] M. Boroson, L. Tutt, K. Nguyen, D. Preuss, M. Culver, G. Phelan, SID Int. Symp. Dig. Tech. Papers. 36 (2005) 972.
[23] T. Hirano, K. Matsuo, K. Kohinata, K. Hanawa, T. Matsumi, E. Matsuda, R. Matsuura, T. Ishibashi, A. Yoshida, T. Sasaoka, SID Int. Symp. Dig. Tech. Papers. 38 (2007) 1592.
[24] S. Lamansky, T.R. Hoffend Jr., H. Le, V. Jones, M.B. Wolk, W.A. Tolbert, Proc. SPIE 5937 (2005) 593702.
[25] J.-R. Gong, L.-J. Wan, S.-B. Lei, C.-L. Bai, X.-H. Zhang, S.-T. Lee, J. Phys. Chem. B 109 (2005) 1675.
[26] C.Y. Kwong, A.B. Djurisic, V.A.L. Roy, P.T. Lai, W.K. Chan, Thin Solid Films 458 (2004) 281.
[27] D. Yokoyama, Y. Setoguchi, A. Sakaguchi, M. Suzuki, C. Adachi, Adv. Funct. Mater. 20 (2010) 386.